THE THREE EXACT COMPONENTS OF THE MAGNETIC FIELD CREATED BY A RADIALLY MAGNETIZED TILE PERMANENT MAGNET

R. Ravaud, G. Lemarquand, V. Lemarquand and C. Depollier

Laboratoire d'Acoustique de l'Universite du Maine
UMR CNRS 6613 Avenue Olivier Messiaen, 72085 Le Mans, France

Abstract—This paper presents the exact analytical formulation of the three components of the magnetic field created by a radially magnetized tile permanent magnet. These expressions take both the magnetic pole surface densities and the magnetic pole volume density into account. So, this means that the tile magnet curvature is completely taken into account. Moreover, the magnetic field can be calculated exactly in any point of the space, should it be outside the tile magnet or inside it. Consequently, we have obtained an accurate 3D magnetic field as no simplifying assumptions have been used for calculating these three magnetic components. Thus, this result is really interesting. Furthermore, the azimuthal component of the field can be determined without any special functions. In consequence, its computational cost is very low which is useful for optimization purposes. Besides, all the other expressions obtained are based on elliptic functions or special functions whose numerical calculation is fast and robust and this allows us to realize parametric studies easily. Eventually, we show the interest of this formulation by applying it to one example: the calculation and the optimization of alternate magnetization magnet devices. Such devices are commonly used in various application fields: sensors, motors, couplings, etc. The point is that the total field is calculated by using the superposition theorem and summing the contribution to the field of each tile magnet in any point of the space. This approach is a good alternative to a finite element method because the calculation of the magnetic field is done without any simplifying assumption.

1. INTRODUCTION

The magnetic field created by arc-shaped permanent magnets can be determined analytically by using three-dimensional [1–17] and two-dimensional approaches [18–23]. Such approaches allow us to realize parametric studies easily since their computational cost is very low. In ironless structures, the magnetic field can be modelled by using equally the Green's function or the Coulombian Model. The analytical expressions obtained are often based on special functions (elliptic functions, Lambad's function). In this paper we show that the azimuthal component created by a tile permanent magnet can be determined without using any special functions. We also proposed semi-analytical expressions for the radial and axial components based on special functions. The point is that we give an exact formulation of the three components of the magnetic field created by a radially magnetized tile permanent magnet. Moreover, these expressions take both the magnetic pole surface densities and the magnetic pole volume density into account. This means that the tile magnet curvature is completely taken into account. Furthermore, the magnetic field can be calculated exactly in any point of the space, outside as well as inside the tile magnet. It is noted that all the expressions given in this paper are three-dimensional, that is, we have obtained an accurate three-dimensional field. Eventually, we illustrate how such expressions are useful for studying the radial field created by alternate magnet structures. Indeed, such structures are very common in various applications such as sensors, motors or magnetic couplings. The expressions given in this paper are available online [37].

2. NOTATION AND GEOMETRY

The geometry considered and the related parameters are shown in Fig. 1. The tile inner radius is r_1; the tile outer radius is r_2; its height is $h = z_2 - z_1$ and its angular width is $\theta_2 - \theta_1$. Calculations are obtained by using the Coulombian model. Consequently, we must take into account the magnetic pole surface densities located on the inner and outer faces of the tile and the magnetic pole volume density located in the tile permanent magnet. The elementary magnetic field $d\mathbf{H}(r, \theta, z)$ can be expressed as follows:

$$d\mathbf{H}(r, \theta, z) = \frac{\sigma^*}{\mu_0} \left(\nabla G(r, r_1) r_1 + \frac{\nabla G(r, r_1)}{r_i} r_i dr_i - \nabla G(r, r_2) r_2 \right) d\theta_i dz_i$$
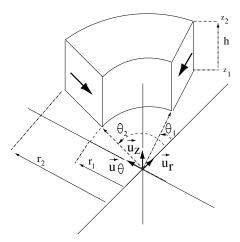
(1)

Figure 1. Representation of the geometry considered. The tile inner radius is r_1; the tile outer radius is r_2; its height is $h = z_2 - z_1$ and its angular width is $\theta_2 - \theta_1$.

where $G(r, r_j)$ is the Green's function defined by

$$G(r, r_j) = \frac{1}{4\pi\sqrt{r^2 + r_j^2 - 2rr_j\cos(\theta - \theta_i) + (z - z_i)^2}} \quad (2)$$

and σ^* corresponds to the fictitious magnetic pole density. Eqs. (1) and (2) are equivalent to the Coulombian model since our structure is ironless.

3. THREE-DIMENSIONAL EXPRESSIONS OF THE MAGNETIC FIELD COMPONENTS

The three magnetic field components can be obtained by calculating the projection of the magnetic field $\mathbf{H}(r, \theta, z)$ along the three defined axes $\vec{u}_r$, $\vec{u}_\theta$ and $\vec{u}_z$. We obtain the magnetic components $H_r(r, \theta, z)$, $H_\theta(r, \theta, z)$ and $H_z(r, \theta, z)$. It is noted that the azimuthal component $H_\theta(r, \theta, z)$ is fully analytical whereas the radial and axial components use elliptic integrals.

3.1. Radial Component $H_r(r, \theta, z)$

The radial component $H_r(r, \theta, z)$ is given by

$$H_r(r, \theta, z) = \sum_{i=1}^{2} \sum_{j=1}^{2} \sum_{k=1}^{2} (-1)^{(i+j+k-1)} \left(S_{i,j,k}^r + V_{i,j,k}^r \right)$$
$$+ \sum_{i=1}^{2} \sum_{j=1}^{2} (-1)^{(i+j)} \mathbf{N_{i,j}} \tag{3}$$

where

$$S_{i,j,k}^r = \alpha_{i,j}^{(0)} \left(\alpha_i^{(1)} \mathbf{F}^* \left[\alpha_{i,j,k}^{(2)}, \alpha_{i,k}^{(3)} \right] + \alpha_i^{(4)} \Pi^* \left[\alpha_{i,j,k}^{(2)}, \alpha_{i,k}^{(5)}, \alpha_{i,k}^{(6)} \right] \right) \tag{4}$$

and

$$V_{i,j,k}^r = -\frac{f \left(z - z_j, r^2 + r_i^2 + (z - z_j)^2, 2rr_i, \cos(\theta - \theta_k) \right)}{\left(\beta^{(1)} + \beta^{(2)} \right)} \tag{5}$$

The function $f(a, b, c, u)$ verifies:

$$f(a, b, c, u) = \beta^{(3)} \left[(b - c) \mathbf{E}^* \left[\beta^{(4)}, \beta^{(5)} \right] + c \mathbf{F}^* \left[\beta^{(4)}, \beta^{(5)} \right] \right]$$
$$+ \beta^{(6)} \left[\left(b - a^2 \right) \mathbf{F}^* \left[\beta^{(7)}, \beta^{(8)} \right] \right] - \beta^{(10)} - \beta^{(11)}$$
$$+ \beta^{(6)} \left[\left(b - a^2 + c \right) \Pi^* \left[\beta^{(9)}, \beta^{(7)}, \beta^{(8)} \right] \right] \tag{6}$$

$$\mathbf{N_{i,j}} = \int_{\cos(\theta - \theta_1)}^{\cos(\theta - \theta_2)} \left(1 - u^2 \right) \arctan \left[\frac{(r_i - ru)(z - z_j)}{\sqrt{r^2 (u^2 - 1) \xi_1}} \right] du \tag{7}$$

with

$$\xi_1 = \sqrt{r^2 + r_i^2 - 2rr_i u + (z - z_j)^2} \tag{8}$$

and the special functions $\mathbf{E}^*$, $\mathbf{F}^*$ and Π^* are the elliptic functions.

3.2. Azimuthal Component $H_\theta(r, \theta, z)$

The azimuthal component $H_\theta(r, \theta, z)$ is given by:

$$H_\theta(r, \theta, z) = \sum_{i=1}^{2} \sum_{j=1}^{2} \sum_{k=1}^{2} (-1)^{(i+j+k-1)} \left(S_{i,j,k}^\theta + V_{i,j,k}^\theta \right) \tag{9}$$

Table 1. Parameters used for calculating the radial component $H_r(r, \theta, z)$.

Parameters	
$\alpha_{i,j}^{(0)}$	$\dfrac{J\sqrt{2}}{4\pi\mu_0} \dfrac{r_i(-z+z_j)}{(2r_i r)^{3/2}\alpha_i^{(1)}}$
$\alpha_i^{(1)}$	$r_i^2 + r^2 + 2r_i r$
$\alpha_{i,j,k}^{(2)}$	$\cos\left(\dfrac{\theta-\theta_k}{2}\right)\sqrt{\dfrac{4r_i r}{\alpha_i^{(1)}+(z-z_j)^2}}$
$\alpha_{i,k}^{(3)}$	$\sqrt{\dfrac{\alpha_i^1+(z-z_j)^2}{4r_i r}}$
$\alpha_i^{(4)}$	$2r_i r^2 - r_i(r_i^2 + r^2)$
$\alpha_{i,k}^{(5)}$	$\dfrac{\alpha_i^{(1)}+(z-z_j)^2}{\alpha_i^{(1)}}$
$\alpha_{i,k}^{(6)}$	$\sqrt{\dfrac{2(\alpha_i^{(1)}+(z-z_j)^2)}{4r_i r}}$
$\beta^{(1)}$	$a\sqrt{1-u^2}\sqrt{\dfrac{b-cu}{b+c}} + \dfrac{a\sqrt{c(1+u)}}{c\sqrt{1-u^2}}$
$\beta^{(2)}$	$\dfrac{a(a^2+b)\arcsin[u]}{c\sqrt{b+c}}\sqrt{b-cu}$
$\beta^{(3)}$	$(1+u)\sqrt{\dfrac{c(u-1)}{b-c}}$
$\beta^{(4)}$	$\arcsin\left[\sqrt{\dfrac{b-cu}{b+c}}\right]$
$\beta^{(5)}$	$\dfrac{b+c}{b-c}$
$\beta^{(6)}$	$\sqrt{1-u^2}\sqrt{\dfrac{c(1+u)}{b+c}}$
$\beta^{(7)}$	$\arcsin\left[\sqrt{\dfrac{1+u}{2}}\right]$
$\beta^{(8)}$	$\dfrac{2c}{b+c}$
$\beta^{(9)}$	$\dfrac{2c}{b+c-a^2}$
$\beta^{(10)}$	$-2\sqrt{1-u^2}\log[a+\sqrt{b-cu}]$
$\beta^{(11)}$	$-\dfrac{\sqrt{x}}{c}\log\left[\dfrac{4c^2\left(c+a^2u-bu+\sqrt{x}\sqrt{1-u^2}\right)}{x^{1.5}(a^2-b+cu)}\right]$
x	$-a^4 + 2a^2 b - b^2 + c$
α	$r_i - r\cos(\theta-\theta_k)$
ξ	$\sqrt{r^2 + r_i^2 + (z-z_j)^2 - 2rr_i\cos(\theta-\theta_k)}$

where

$$S^{\theta}_{i,j,k} = -\frac{(z - z_j)}{r\sqrt{-(z - z_j)^2}} \arctan\left[\frac{\xi_2}{\sqrt{-(z - z_j)^2}}\right] \qquad (10)$$

with

$$\xi_2 = \sqrt{r_i^2 + r^2 + (z - z_j)^2 - 2rr_i\cos(\theta - \theta_k)} \qquad (11)$$

and

$$\begin{aligned}
V^{\theta}_{i,j,k} &= \frac{1}{r}\left(-z_j - \alpha\log\left[z - z_j + \xi\right] + (z - z_j)\log\left[\alpha + \xi\right]\right) \\
&\quad + \sin(\theta - \theta_k)\arctan\left[\frac{r\sin(\theta - \theta_k)}{z - z_j}\right] \\
&\quad + \sin(\theta - \theta_k)\arctan\left[\frac{(z - z_j)\alpha}{r\sin(\theta - \theta_k)\xi}\right] \qquad (12)
\end{aligned}$$

It is emphasized here that the azimuthal component expression is fully analytical, that is, it does not use any special functions.

3.3. Axial Component $H_z(r, \theta, z)$

The axial component $H_z(r, \theta, z)$ is given by:

$$H_z(r, \theta, z) = \sum_{i=1}^{2}\sum_{j=1}^{2}\sum_{k=1}^{2}(-1)^{(i+j+k-1)}\left(S^z_{i,j,k}\right) + \sum_{i=1}^{2}\sum_{j=1}^{2}(-1)^{(i+j)}V^z_{i,j} \qquad (13)$$

with

$$S^z_{i,j,k} = \frac{2r_i}{(r - r_i)^2 + (z - z_j)^2}\mathbf{F}\left[\frac{\theta - \theta_k}{2}, -\frac{4rr_i}{(r - r_i)^2 + (z - z_j)^2}\right] \qquad (14)$$

and

$$V^z_{i,j} = \int_{\theta_1}^{\theta_2}\tanh^{-1}\left[\frac{\sqrt{r^2 + r_i^2 + (z - z_j)^2 - 2rr_i\cos(\theta - \theta_s)}}{r_i - r\cos(\theta - \theta_s)}\right]d\theta_s \qquad (15)$$

4. THREE-DIMENSIONAL STUDY OF THE RADIAL FIELD CREATED BY ALTERNATE MAGNET STRUCTURES

Alternate magnet structures are commonly used in electrical machines for creating a radial field, in magnetic couplings or in magnetic sensors. The way of assembling tile permanent magnets depends greatly on the intended application. Let us first consider an assembly of tile permanent magnets radially magnetized (Fig. 2). Each tile angular width is $\frac{\pi}{4}$ rad. Thus, the geometry owns four pairs of poles. We represent in Fig. 3 the radial field created by such a geometry for three radial distances r and in Fig. 4 its three-dimensional representation. We see here that it is very important to use a three-dimensional approach for precisely calculating the magnetic field created by arc-shaped permanent magnets. Moreover, the time necessary for representing the three-dimensional representation is very low (a few seconds).
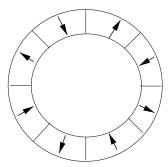

Figure 2. Representation of an alternate magnet structures with 4 pairs of poles.

In addition, Fig. 3 clearly shows that such an approach can be used for studying an ABS sensor as such a sensor generally uses alternate magnets. Indeed, in such a sensor, the number of tiles used is an important parameter as an increase in the number of tiles can generate a decrease in the magnetic field magnitude. Consequently, only the 3D analytical approach allows us to know the number of tiles necessary to optimize the dimensions of an ABS sensor. More generally, as the computational cost is very low, we can easily change the tile dimensions in order to create another radial field. Let us consider an alternate magnet structure whose tiles are all radially magnetized but have not the same angular width. For example, let us consider the case when the first pole (north pole) has an angular width which equals $\frac{\pi}{4}$, the
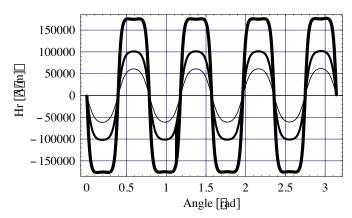
Figure 3. Representation of the radial field created by an alternate magnet structure: the angular width of a tile is $\frac{\pi}{4}$; the inner radius is 0.025 m; the outer radius is 0.028 m; the height is 0.003 m and $J = 1$ T; the more H_r is calculated far from the alternate magnet structure, the thinner is the line represented in this figure ($r = 0.024$ m, $r = 0.023$ m, $r = 0.022$ m), $z = 0.001$ m.
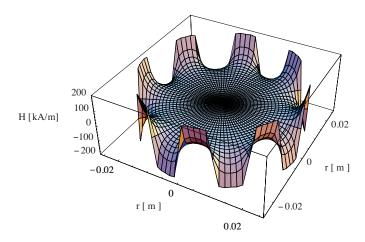

Figure 4. Three-dimensional representation of the radial field created by an alternate magnet structure: the angular width of a tile is $\frac{\pi}{4}$; the inner radius is 0.025 m; the outer radius is 0.028 m; the height is 0.003 m and $J = 1$ T; the more H_r is calculated far from the alternate magnet structure, the thinner is the line represented in this figure ($r = 0.024$ m, $r = 0.023$ m, $r = 0.022$ m), $z = 0.001$ m.
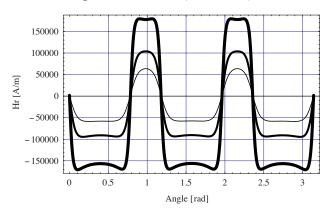
Figure 5. Representation of the radial field created by an alternate magnet structure whose tile permanent magnets have not the same angular width: We have $\theta_2 - \theta_1 = \frac{\pi}{8}$ and $\theta_2 - \theta_1 = \frac{\pi}{4}$; the inner radius is $0.025\,\mathrm{m}$; the outer radius is $0.028\,\mathrm{m}$; the height is $0.003\,\mathrm{m}$ and $J = 1\,\mathrm{T}$; the more H_r is calculated far from the alternate magnet structure, the thinner is the line represented in this figure ($r = 0.024\,\mathrm{m}$, $r = 0.023\,\mathrm{m}$, $r = 0.022\,\mathrm{m}$), $z = 0.001\,\mathrm{m}$.
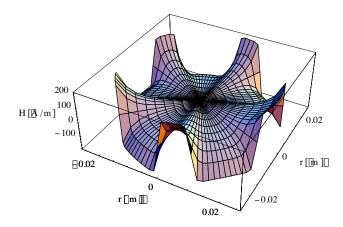

Figure 6. Three-dimensional representation of the radial field created by an alternate magnet structure whose tile permanent magnets have not the same angular width: We have $\theta_2 - \theta_1 = \frac{\pi}{8}$ and $\theta_2 - \theta_1 = \frac{\pi}{4}$; the inner radius is $0.025\,\mathrm{m}$; the outer radius is $0.028\,\mathrm{m}$; the height is $0.003\,\mathrm{m}$ and $J = 1\,\mathrm{T}$; the more H_r is calculated far from the alternate magnet structure, the thinner is the line represented in this figure ($r = 0.024\,\mathrm{m}$, $r = 0.023\,\mathrm{m}$, $r = 0.022\,\mathrm{m}$), $z = 0.001\,\mathrm{m}$.

second tile (the south pole) has an angular width which equals $\frac{2\pi}{4}$, and this configuration is repeated around the ring. We represent in Figs. 5 and 6 a radial field both in two and three dimensions. Here again, the time necessary for plotting the three-dimensional radial field is very low. Fig. 5 shows an interesting point. We can see that the more the radial field is calculated far from the magnets, the more it is uniform in front of the magnets whose angular width equals $\frac{2\pi}{8}$. This result is interesting because some applications do not often require a great radial field but rather a uniform radial field on a given angular space. We see here that this radial field is not uniform, neither close to but rather far from the magnets.

5. CONCLUSION

This paper has presented new three-dimensional expressions of the magnetic field created by tile permanent magnets. In addition, we have presented a fully analytical expression of the azimuthal component. As both the surface densities and the volume density are taken into account for calculating the magnetic field components, all their expressions are exact for all points in space, outside as well as inside the magnet. So, this means that the tile magnet curvature is fully taken into account, without any simplifying assumption. For example, these expressions allow us to study the magnetic field created by alternate magnet structures. Indeed, these structures are commonly used in many applications such as magnetic sensors, permanent magnet motors or magnetic couplings. So, their design and their optimization can be easily realized with such an approach as the presented expressions have a very low computational cost. We can say that such a three-dimensional approach is a good alternative to a classical finite-element method. The expressions given in this paper are available online [37].

REFERENCES

1. Babic, S. and C. Akyel, "Improvement of the analytical calculation of the magnetic field produced by permanent magnet rings," *Progress In Electromagnetics Research*, PIER 5, 71–82, 2008.
2. Ravaud, R., G. Lemarquand, V. Lemarquand, and C. Depollier, "Analytical calculation of the magnetic field created by permanent-magnet rings," *IEEE Trans. Magn.*, Vol. 44, No. 8, 1982–1989, 2008.
3. Selvaggi, J., S. Salon, O. M. Kwon, and M. Chari, "Computation of the three-dimensional magnetic field from solid permanent-

magnet bipolar cylinders by employing toroidal harmonics," *IEEE Trans. Magn.*, Vol. 43, No. 10, 3833–3839, 2007.

4. Azzerboni, B. and G. Saraceno, "Three-dimensional calculation of the magnetic field created by current-carrying massive disks," *IEEE Trans. Magn.*, Vol. 34, No. 5, 2601–2604, 1998.

5. Conway, J., "Inductance calculations for noncoaxial coils using bessel functions," *IEEE Trans. Magn.*, Vol. 43, No. 3, 1023–1034, 2007.

6. Rakotoarison, H. L., J. P. Yonnet, and B. Delinchant, "Using coulombian approach for modeling scalar potential and magnetic field of a permanent magnet with radial polarization," *IEEE Trans. Magn.*, Vol. 43, No. 4, 1261–1264, 2007.

7. Durand, E., "Electrostatique," *Masson Editeur, Paris, France*, Vol. 1, 248–251, 1964.

8. Babic, S. and C. Akyel, "Magnetic force calculation between thin coaxial circular coils in air," *IEEE Trans. Magn.*, Vol. 44, No. 4, 445–452, 2008.

9. Babic, S., C. Akyel, and S. Salon, "New procedures for calculating the mutual inductance of the system: Filamentary circular coil-massive circular solenoid," *IEEE Trans. Magn.*, Vol. 39, No. 3, 1131–1134, 2003.

10. Babic, S., C. Akyel, S. Salon, and S. Kincic, "New expressions for calculating the magnetic field created by radial current in massive disks," *IEEE Trans. Magn.*, Vol. 38, 497–500, March 2002.

11. Babic, S., C. Akyel, S. Salon, and S. Kincic, "New expressions for calculating the magnetic field created by radial current in massive disks," *IEEE Trans. Magn.*, Vol. 38, No. 2, 497–500, 2002.

12. Babic, S., S. Salon, and C. Akyel, "The mutual inductance of two thin coaxial disk coils in air," *IEEE Trans. Magn.*, Vol. 40, No. 2, 822–825, 2004.

13. Conway, J., "Noncoaxial inductance calculations without the vector potential for axisymmetric coils and planar coils," *IEEE Trans. Magn.*, Vol. 44, No. 10, 453–462, 2008.

14. Furlani, E. P. and S. Reznik, and A. Kroll, "A three-dimensional field solution for radially polarized cylinders," *IEEE Trans. Magn.*, Vol. 31, No. 1, 844–851, 1995.

15. Furlani, E., "Field analysis and optimization of ndfeb axial field permanent magnet motors," *IEEE Trans. Magn.*, Vol. 33, No. 5, 3883–3885, 1997.

16. Furlani, E. and M. Knewston, "A three-dimensional field solution for permanent-magnet axial-field motors," *IEEE Trans. Magn.*,

Vol. 33, No. 1, 2322–2325, 2008.

17. Furlani, E. P., *Permanent Magnet and Electromechanical Devices: Materials, Analysis and Applications*, 235–245, Academic Press, 2001.

18. Furlani, E. P., "A two-dimensional analysis for the coupling of magnetic gears," *IEEE Trans. Magn.*, Vol. 33, No. 3, 2317–2321, 1997.

19. Mayergoyz, D. and E. P. Furlani, "The computation of magnetic fields of permanent magnet cylinders used in the electrophotographic process," *J. Appl. Phys.*, Vol. 73, No. 10, 5440–5442, 1993.

20. Azzerboni, B. and E. Cardelli, "Magnetic field evaluation for disk conductors," *IEEE Trans. Magn.*, Vol. 29, No. 6, 2419–2421, 1993.

21. Azzerboni, B., E. Cardelli, M. Raugi, A. Tellini, and G. Tina, "Magnetic field evaluation for thick annular conductors," *IEEE Trans. Magn.*, Vol. 29, No. 3, 2090–2094, 1993.

22. Yonnet, J. P., "Passive magnetic bearings with permanent magnets," *IEEE Trans. Magn.*, Vol. 14, No. 5, 803–805, 1978.

23. Yonnet, J. P., "Permanent magnet bearings and couplings," *IEEE Trans. Magn.*, Vol. 17, No. 1, 1169–1173, 1981.

24. Yonnet, J. P., *Rare-earth Iron Permanent Magnets*, Ch. Magnetomechanical devices, Oxford Science Publications, 1996.

25. Blache, C. and G. Lemarquand, "Linear displacement sensor with hight magnetic field gradient," *Journal of Magnetism and Magnetic Materials*, Vol. 104, 1106–1108, 1992.

26. Blache, C. and G. Lemarquand, "New structures for linear displacement sensor with hight magnetic field gradient," *IEEE Trans. Magn.*, Vol. 28, No. 5, 2196–2198, 1992.

27. Zhu, Z. and D. Howe, "Analytical prediction of the cogging torque in radial-field permanent magnet brushless motors," *IEEE Trans. Magn.*, Vol. 28, No. 2, 1371–1374, 1992.

28. Wang, J., G. W. Jewell, and D. Howe, "Design optimisation and comparison of permanent magnet machines topologies," *IEE Proc. Elect. Power Appl.*, Vol. 148, 456–464, 2001.

29. Halbach, K., "Design of permanent multiple magnets with oriented rec material," *Nucl. Inst. Meth.*, Vol. 169, 1–10, 1980.

30. Abele, M., J. Jensen, and H. Rusinek, "Generation of uniform high fields with magnetized wedges," *IEEE Trans. Magn.*, Vol. 33, No. 5, 3874–3876, 1997.

31. Aydin, M., Z. Zhu, T. Lipo, and D. Howe, "Minimization of cogging torque in axial-flux permanent-magnet machines: Design

concepts," *IEEE Trans. Magn.*, Vol. 43, No. 9, 3614–3622, 2007.

32. Marinescu, M. and N. Marinescu, "Compensation of anisotropy effects in flux-confining permanent-magnet structures," *IEEE Trans. Magn.*, Vol. 25, No. 5, 3899–3901, 1989.

33. Akoun, G. and J. P. Yonnet, "3D analytical calculation of the forces exerted between two cuboidal magnets," *IEEE Trans. Magn.*, Vol. 20, No. 5, 1962–1964, 1984.

34. Yong, L., Z. Jibin, and L. Yongping, "Optimum design of magnet shape in permanent-magnet synchronous motors," *IEEE Trans. Magn.*, Vol. 39, No. 11, 3523–4205, 2003.

35. Lemarquand, G. and V. Lemarquand, "Annular magnet position sensor," *IEEE. Trans. Magn.*, Vol. 26, No. 5, 2041–2043, 1990.

36. Lemarquand, G., "A variable reluctance sensor," *IEEE Trans. Magn.*, Vol. 25, No. 5, 3827–3829, 1989.

37. http://www.univ-lemans.fr/∼glemar.